SUPPLEMENTARY MATERIALS

The controversial role of ascorbic acid in boosting the performance of heterogeneous Fenton-like catalysts for wastewaters treatment: The case study of $Fe_2V_4O_{13}$

Arshitha Madhusudhan[a,b], Sridhar Gowrisankaran[a], František Zažímal[c], Leonid Satrapinskyy[d], Tomaš Roch[d], Tomaš Homola[c], Dana Dvoranova[e], Marcello Brigante[b], Olivier Monfort[a,d]*

[a.] *Department of Inorganic Chemistry, Faculty of Natural Sciences, Comenius University Bratislava, Ilkovicova 6, Mlynska Dolina, 84215 Bratislava, Slovak Republic.*

[b.] *Université Clermont Auvergne, CNRS, Institut de Chimie de Clermont-Ferrand, Clermont-Ferrand, F-63000, France.*

[c.] *Department of Plasma Physics and Technology, Faculty of Science, Masaryk University, Kotlářská 267/2, 602 00 Brno, Czech Republic.*

[d.] *Center for Nanotechnology and Advanced Materials, Faculty of Mathematics Physics and Informatics, Comenius University Bratislava, Mlynska dolina, 84248 Bratislava, Slovak Republic.*

[e.] *Institute of Physical Chemistry and Chemical Physics, Faculty of Chemical and Food Technology, Slovak University of Technology in Bratislava, Radlinskeho 9, 81237 Bratislava, Slovak Republic*

Text S1: LC-MS analysis

The identification of SMX degradation products was performed by an ultra-high performance liquid chromatography coupled to high-resolution mass spectrometry performed on an Orbitrap Q-Exactive (Thermo scientific). The column was a Phenomenex Kinetex C18 (1.7 µm × 100 Å; 100 × 2.1 mm) and the temperature was fixed at 30°C. The initial mixture of eluents was 5% acetonitrile and 95% water acidified with 0.1% formic acid, followed by a linear gradient to 99% acetonitrile within 8.5 min and held for 1 min. The flow rate was 0.45 mL min^{-1} and the injection volume was 5 µL. Ionization was set to 3.2 kV (ESI+) and 3.0 kV (ESI).

Text S2: Scavenging experiments

To determine the suitable concentration of scavengers for the selected reactive oxygen species (ROS), second-order rate constants between targeted RS and the scavenger ($k_{RS,scav.}$) and targeted ROS and SMX ($k_{RS,SMX}$) were considered (Table S1). The amount of the selected ROS which is scavenged (Q in %) is calculated based on the following equation:

$$Q = \frac{c_{scav.} \cdot k_{RS,scav.}}{c_{scav.} \cdot k_{RS,scav.} + C_{SMX} \cdot k_{RS,SMX}}$$

where $c_{scav.}$ and c_{SMX} are the initial concentrations of the scavenger and SMX, respectively. In our work, we have used 5 mM TBA, 20 mM IPA and 5 mM FFA, thus scavenging 91% of $^{\bullet}OH$, 85%-96% of $^{\bullet}OH$ and $SO_4^{\bullet -}$, and 99% of $^1O_2$. It is worth noting FFA can also quench significantly $^{\bullet}OH$ and $SO_4^{\bullet -}$, so FFA is used in combination with IPA.

Text S3: Optimization of AA and PS concentrations

The effects of AA and PS concentrations on SMX degradation were investigated both in the dark and under UVA radiation (Fig. S2). As the AA concentration increased from 0.10 – 0.25 mM, the removal efficiency of SMX increased also, before to decrease in the range 0.25 – 1.00 mM. The effect of light is significant as the SMX degradation reached 60% after 3 h under UVA light compared to 30% in the dark. Since AA is an reducing agent, it is helping in the (re)generation of Fe(II) from Fe(III), thus increasing the efficiency of Fenton-based processes. However, an excess of AA can lead to decrease of the degradation performance as this antioxidant can scavenge generated ROS. On the other hand, a constant increase of the PS concentration (from 0.5 mM to 5.0 mM) leads to higher performance in SMX degradation. There is also a positive impact of the UVA light as PS can be activated by both photocatalysis or Fenton-based processes. Since high PS concentration cannot be considered economically viable for potential applications, we consider concentrations of 0.25 mM AA and 2.0 mM PS in the rest of the present study.

The effect of AA and PS were investigated both in dark and UVA irradiation. Figure S2a shows the degradation of SMX with varying concentration of AA with PS kept constant (2 mM). It is worth noting that the degradation of SMX the removal efficiency increases with increasing concentration and decreases as the concentration increased to 0.5 mM. Although ascorbic acid (AA) acts as a reducing agent that accelerates the Fenton reaction by enhancing the redox cycle, it is also a strong antioxidant that can scavenge reactive radicals, which may lead to consumption of radicals. Experiment using different PS concentration from 0.5 to 5.0 mM shows that increasing in degradation efficiency of SMX as the concentration of PS which is in converse with the addition of AA (Figure S2b).

Text S4: Identification of SMX degradation products by LC-MS

SMX has a peak at $[M+H]^+$ = 254.0589 with sodium adduct $[M+Na]^+$ = 276.0407 and [M-H]- = 252.0437. The product P1 was generated by oxidation of the double bond on the aromatic ring. P2 and P3 were identified as products of the sulphonamide bond cleavage by hydroxyl radical leading to the formation the 3-amino-5-methylisoxazole and sulfanilic acid (Fig. S5). Products P4, P5 derived from P1 isoxazole ring opening and further oxidation of aromatic ring.

Table S1: Ascorbic acid based heterogenous Fenton systems

Catalyst (dosage)	**Oxidant (conc.)**	**Pollutant (conc.)**	**AA conc.**	**Performance without AA (%)**	**Performance with AA (%)**	**Refs**
Iron silicate (0.3 g/L)	$S_2O_8^{-2}$ (1.0 mM)	Sulfamethazine (2.5 mg/L)	0.5 mM	~ 20	90	[1]
$Fe@Fe_2O_3$ (0.1 g/L)	H_2O_2 (1.0 mM)	Alachlor (74 µM)	1.0 mM	~10	100	[2]
Fe_3O_4 (1g/L)	H_2O_2 (1.0 mM)	Alachlor (20 mg/L)	0.5mM	~10	75	[3]
Silicate-iron	H_2O_2 (2.5 mM)	p-nitrophenol (100 mg/L)	1.0 mM	~ 15	89	[4]
Fe^{3+} (0.2 mM)	H_2O_2 (2.0 mM)	Alachlor (100 µM)	0.2 mM	~40	100	[5]
$Fe_2V_4O_{13}$ (0.5g/L)	$S_2O_8^{-2}$ (0.5 mM)	Sulfamethoxazole (40 µM)	0.25 mM	17	55	This work

Table S2: Second order rate constants of SMX and scavengers with different reactive oxygen species (ROS).

Chemicals	$k_{\bullet OH}$ ***[M⁻¹S⁻¹]***	$k_{SO_4^{\bullet -}}$ ***[M⁻¹S⁻¹]***	$k_{^1O_2}$ ***[M⁻¹S⁻¹]***	***Reference***
Sulfamethoxazole	6.98×10^9	2.98×10^9	1.34×10^6	[6,7]
Tert-butanol	6.0×10^8	8.4×10^5	-	[8,9]
Isopropyl alcohol	8.2×10^7	1.9×10^8	-	[8,10]
Furfuryl alcohol	1.5×10^{10}	-	1.2×10^8	[11]

Table S3: EDX analysis of FVO.

	at.%
C	4.63
O	33.64
V	42.72
Fe	19.01

Table S4: The elemental concentration of FVO determined by XPS analysis (expressed in at. %).

	Fe	*V*	*O*	*C*	*N*	Fe_{adC}	V_{adC}	O_{adC}	Fe_{FVO}	V_{FVO}	O_{FVO}
FVO	8.7	18.6	48.8	22.7	1.0	11.4	24.4	64.2	12.0	25.8	62.2

Table S5: Comparison of Iron vanadate catalyst performance to this work

Catalyst (dosage)	**Oxidant (conc.)**	**Pollutant (conc.)**	**Conditions**	**Deg. Perf. (%)**	**RSE values**	**Refs**
$FeVO_4$ (0.8 g/L)	HSO_5^- (1.0 mM)	Oxytetracycline (20 mg/L)	pH 6, dark, 40min	100	0.108	[12]
Fe_2O_3/V_2O_5/BC (0.2 g/L)	HSO_5^- (100 mM)	Tetracycline (10 mg/L)	pH 3, light, 120min	99.58	0.0002	[13]
$FeVO_4\cdot 1.1H_2O$ (0.5 g/L)	HSO_5^- (2 mM)	Methylene blue (20 μM)	pH 4, light, 60min	98	0.0098	[14]
Self-doped $FeVO_4$ (0.5 g/L)	HSO_5^- (0.4 mM)	Sulfamethoxazole (0.02mM)	pH 5.41, light, 60 min	96.6	0.0477	[15]
α-$Fe_2O_3/V_2O_5/MoS_2$ (1g/L)	-	Tetracycline hydrochloride, (20.79 μM)	pH 7.4, dark, 120min	86	-	[16]
$MoS_2/FeVO_4$ (1 g/L)	H_2O_2 (98 mM)	Tetracycline (50mg/L)	pH 4, light, 60 min	72	0.0016	[17]
$Fe_2V_4O_{13}$ (0.5g/L)	H_2O_2 (15 mM)	Acid Orange II	pH 6, light, 30min	68.7	-	[18]
$Fe_2V_4O_{13}$ (0.5g/L)	HSO_5^- (0.5 mM)	Sulfamethoxazole (40 μM)	light, 180min	55	0.323	This work

Table S6: SMX and degradation products detected by LC-MS

Compound	Rt *(min)*	Exp *$[M+H]^+$*	Theor *$[M+H]^+$*	Δmu	Exp *$[M-H]^-$*	Théor *$[M-H]^-$*	Δm mu	Molecular formula	Proposed Structure
SMX	2.80	254.0589 276.0407 *$[M+Na]^+$*	254.0594	0.45	252.0443	252.0437	0.56	$C_{10}H_{11}N_3O_3S$	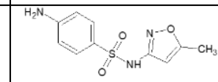
P1	2.64	270.0535	270.0543	0.78	268.0396	268.0387	0.94	$C_{10}H_{11}N_3O_4S$	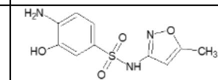
P2	1.83				172.0064	172.0063	0.08	$C_6H_7NO_3S$	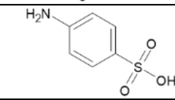
P3	0.84	99.0556	99.0553	0.31				$C_4H_6N_2O$	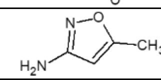
P4	1.08	272.0693	272.0700	0.63				$C_{10}H_{13}N_3O_4S$	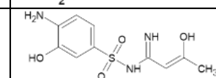
P5	0.90	288.0643	288.0649	0.59				$C_{10}H_{13}N_3O_5S$	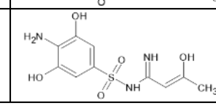

Table S7: The elemental concentration of FVO after the experiment determined by XPS analysis (expressed in at. %).

	C	*F*	*Fe*	*K*	*N*	*O*	*S*	*V*	*Fe_{adC}*	*V_{adC}*	*O_{adC}*
FVO after use	16.3	6.7	4.1	4.8	3.3	47.5	3.7	13.7	6.3	21.0	72.7

Table S8: Physicochemical characteristics of tertiary effluents collected at WWTP Bratislava-Petrzalka on 10/10/2023 (data provided by BVS a.s. company - Bratislava Water Company).

Test	*Quantity*
Chemical oxygen demand	26 mg L^{-1}
Biological oxygen demand	3.0 mg L^{-1}
Non-dissolved matter at 105 °C	10.0 mg L^{-1}
Total inorganic nitrogen	9.31 mg L^{-1}

Total phosphor	0.55 mg L^{-1}

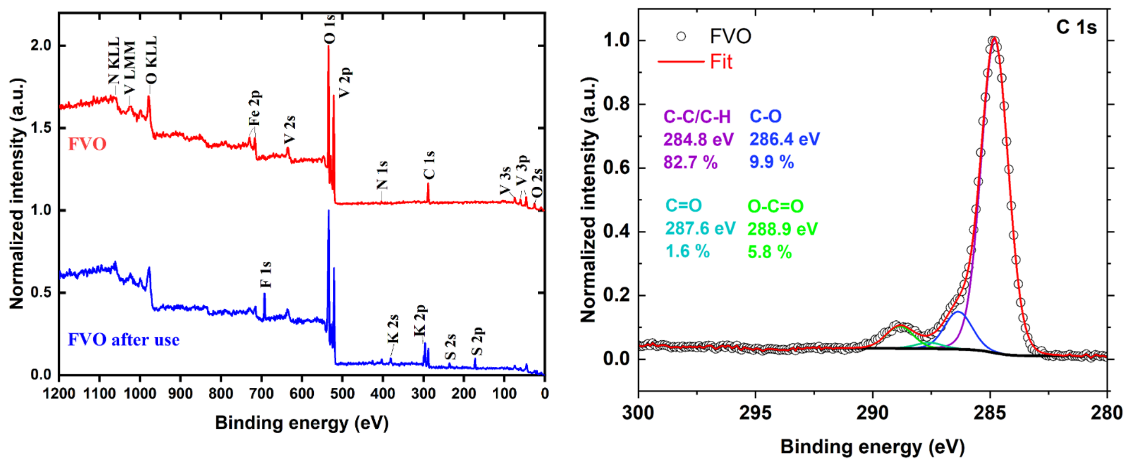

Fig. S1. Survey spectrum and high resolution XPS spectra of FVO demonstrating the presence of C.

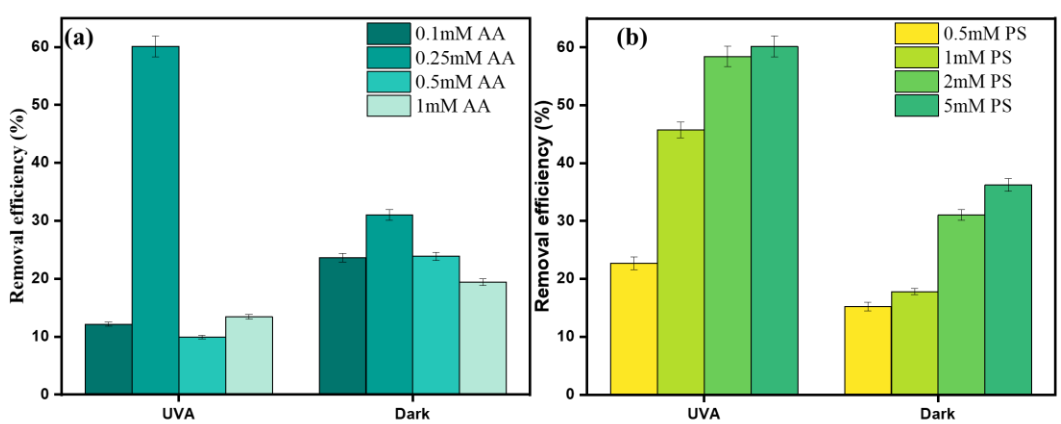

Fig. S2. Effect of AA and PS concentrations on degradation of SMX under dark and light after 3 h reaction (fixed amount of 0.25 mM AA in Fig. S2a and 0.5 mM PS in Fig. S2b)

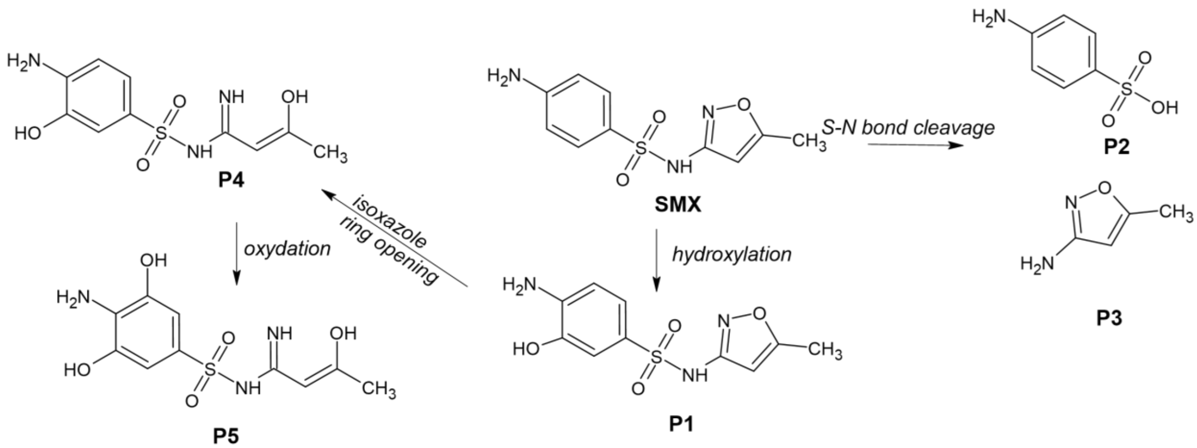

Fig. S3. Proposed degradation pathway of SMX.

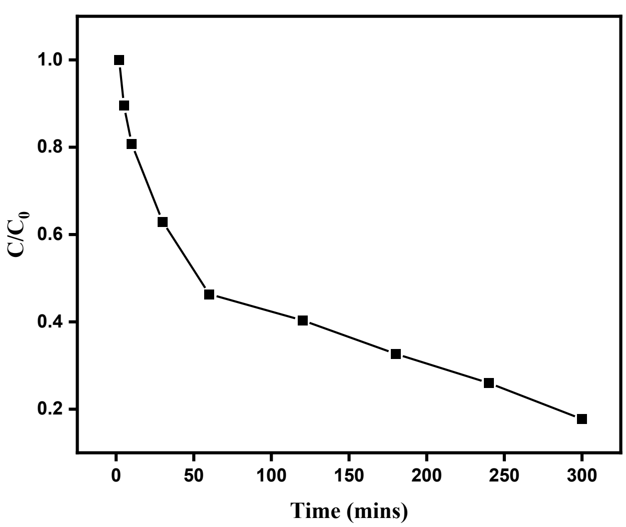

Fig. S4. Consumption of PS over 300min of the degradation of SMX under UVA exposure c_0(PS) 0.5mM.

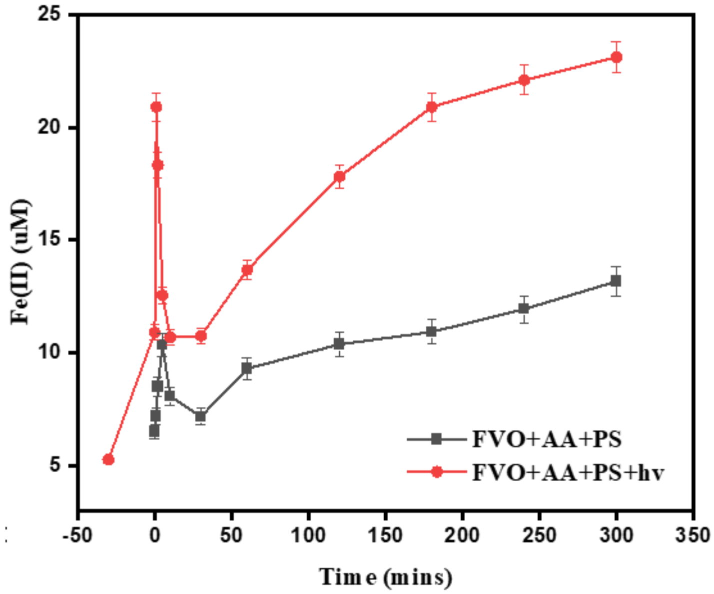

Fig. S5. Iron (II) in the ternary system in dark and upon UVA exposure.

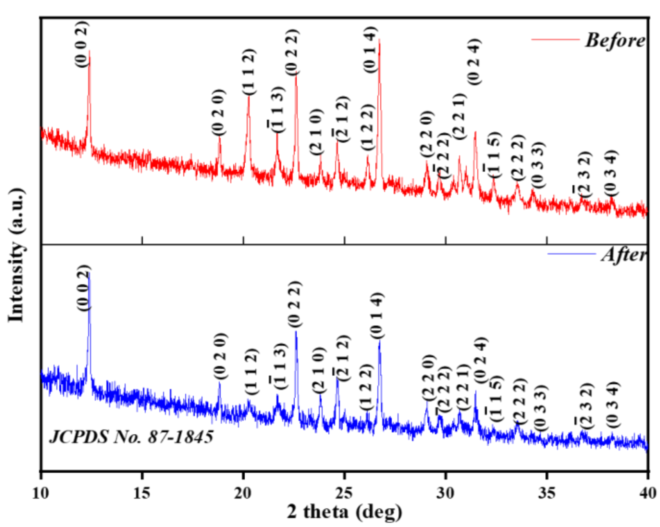

Fig. S6. XRD of FVO before and after use for degradation of SMX.

References

1 Y. Li, H. Dong, J. Xiao, L. Li, Y. Hou, D. Chu, X. Hou, S. Xiang and Q. Dong, *Chemical Engineering Journal*, 2023, 455, 140773.

2 X. Hou, X. Huang, Z. Ai, J. Zhao and L. Zhang, *J. Hazard. Mater.*, 2016, 310, 170–178.

3 H. Sun, G. Xie, D. He and L. Zhang, *Appl. Catal. B*, 2020, 267, 118383.

4 Y. Yuan, J. Shi, W. Xie, G. Wang, Y. Wang, J. Tang and H. Lu, *Colloids Surf. A Physicochem. Eng. Asp.*, 2024, 685, 133307.

5 J. Bolobajev, M. Trapido and A. Goi, *Chemical Engineering Journal*, 2015, 281, 566–574.

6 L. Gao, Q. Mao, S. Luo, L. Cao, X. Xie, Y. Yang, Y. Deng and Z. Wei, *Environmental Pollution*, 2020, 259, 113795.

7 A. M. Lastre-Acosta, B. S. Cristofoli, M. P. S. Parizi, C. A. O. do Nascimento and A. C. S. C. Teixeira, *Environmental Science and Pollution Research*, 2021, 28, 23887–23895.

8 G. V. Buxton, C. L. Greenstock, W. P. Helman and A. B. Ross, *J. Phys. Chem. Ref. Data*, 1988, 17, 513–886.

9 C. L. Clifton and R. E. Huie, *Int. J. Chem. Kinet.*, 1989, 21, 677–687.

10 R. E. Huie, C. L. Clifton and P. Neta, *International Journal of Radiation Applications and Instrumentation. Part*, 1991, 38, 477–481.

11 X. Mi, P. Wang, S. Xu, L. Su, H. Zhong, H. Wang, Y. Li and S. Zhan, *Angewandte Chemie*, 2021, 133, 4638–4643.

12 Y. Tang, J. Kang, M. Wang, C. Jin, J. Liu, M. Li, S. Li and Z. Li, *J. Environ. Chem. Eng.*, 2021, 9, 105864.

13 J. Liu, Y. Zhang, Y. Dong, Z. Jiang, L. Zhang, W. Liu, J. Guan and H. Lin, *Sep. Purif. Technol.*, 2024, 328, 125034.

14 D. Li, Z. Yao, J. Lin, W. Tian, H. Zhang, X. Duan and S. Wang, *J. Environ. Chem. Eng.*, 2022, 10, 107199.

15 J. Zhang, W. Zhao, Z. Li, G. Lu and M. Zhu, *Chemical Engineering Journal*, 2021, 403, 126384.

16 G. Venkatesh, K. Mazen, K. Manimaran, F. Samara and S. Kanan, *Journal of Materials Science 2025 60:31*, 2025, 60, 13413–13434.

17 Q. Liu, J. Zhao, Y. Wang, Y. Liu, J. Dong, J. Xia and H. Li, *Colloids Surf. A Physicochem. Eng. Asp.*, 2021, 623, 126721.

18 Y. Y. Zhang, C. He, J. H. Deng, Y. T. Tu, J. K. Liu and Y. Xiong, *Research on Chemical Intermediates 2009 35:6*, 2009, 35, 727–737.